# NMR studies of biosynthesis and enzyme mechanism

A. Ian Scott

Center for Biological NMR, Department of Chemistry, Texas A&M University, College Station, Texas 77843, U.S.A.

Abstract - Recent applications of high-field NMR spectroscopy in biosynthesis will be discussed. The emphasis of the lecture will be on the use of  $^1\mathrm{H},~^3\mathrm{H},~^{13}\mathrm{C}$  and  $^{15}\mathrm{N}\text{-NMR}$  to focus on individual steps of biochemical processes in the formation of natural products and related enzyme-catalyzed events. In the first set of experiments, pulse labelling and in vivo studies are used to uncover biosynthetic sequences in the porphyrin-corrin pathway. In the second type of NMR experiment, the application of  $^1\mathrm{H}$  and  $^3\mathrm{H}\text{-NMR}$  spectroscopy has illuminated the course of certain key biosynthetic steps in the synthesis of porphyrins and  $\beta$ -lactam antibiotics. These methods have quite general application in biochemical and biological systems. Thirdly, the full magnifying power of the NMR "lens" is used to decipher molecular events during enzyme-catalyzed reactions in solution at subzero temperature and in the solid state.

#### INTRODUCTION

The study of the biosynthesis of natural products has recently been enriched by the application of high-field nuclear magnetic resonance (NMR) spectroscopy to examine the effects of feeding substrates labeled with stable isotopes in such juxtaposition that the timing of the making and breaking of C-C, C-O, C-N and C-H bonds during the assembly of a complex product from its constituent building blocks can frequently be reconstructed by post mortem examination of the target molecule labeled with  $^{13}$ C,  $^{18}$ O,  $^{15}$ N and  $^{2}$ H. These methods depend on direct observation of isotopic shifts ( $^{18}$ O,  $^{2}$ H) on  $^{13}$ C signals, on C-X spin coupling observation and, more recently, by spectral editing and 2-D NMR techniques which, for example, will filter out and edit all  $^{13}\mathrm{C}$  nuclei bound directly to  $^{1}\mathrm{H}$ . We now provide examples of some novel NMR techniques designed to probe the biosynthetic pathway at the <u>single enzyme</u> level. We first discuss a "hidden" pathway where it can be deduced that several methylating enzymes are at work in sequence during the overall transformation of hexa-hydroporphyrin to corrin. Using the nucleus <sup>3</sup>H, we next dissect the stages of the actual encounter of the small substrate, porphobilinogen (PBG), with its enzyme (PBG deaminase), an event which initiates the first part of porphyrin (and corrin) synthesis. Turning to a more common (but still mysterious) class of enzyme-catalyzed reaction, we describe both high-field <sup>1</sup>H and <sup>13</sup>C NMR experiments which have been carefully designed to characterize small, labile product molecules released from enzyme and, more importantly, to detect transient covalent intermediates bound to enzyme, which are part of the catalytic machinery. The high molecular weights of these productive species (~20,000 MW) require extreme rigor in defining the NMR parameters for their detection. An example from a cognate study of stable transition state analog inhibitor complexes will be presented. The technique of cross polarized magic angle spinning (CPMAS) is applied to the study of dynamic turnover in solid enzyme-substrate interactions, thus bridging the gap between X-ray diffraction and NMR analysis of biomolecules. Finally, examples of in vivo, non-invasive <sup>13</sup>C-NMR spectroscopy will be discussed.

## BIOSYNTHESIS OF VITAMIN B<sub>12</sub>: TIMING OF THE METHYLATION STEPS BETWEEN URO'GEN III AND COBYRINIC ACID

The details of the pathway of corrin biosynthesis beyond the key intermediate uro'gen III (1) (ref. 1) are still incomplete. The first three enzymatic steps consist of successive C-methylations of uro'gen III at C-2 (ref. 2), C-7 (ref. 3), and C-20 (ref. 4), and the corresponding intermediates have been isolated in their stable aromatized forms (ref. 5), e.g., the 2,7-dimethyl isobacteriochlorin, sirohydrochlorin (2) and its 20-methyl derivative, Factor III (3). In spite of an intensive search spanning the last ten years (ref. 6), the remaining steps are unknown with respect to isolation of intermediates containing four or more methyl groups (up to a possible of eight) but, as noted previously (ref. 1), the proven biochemical conversion of Factor III (3) to cobyrinic acid (4) must involve the following events (see Scheme 1), not necessarily in the order indicated: (i) The successive addition

#### Scheme 1

Uro'gen III

Sirohydrochlorin (Factor II) 
$$R = H$$

Factor III

 $RO_2C$ 
 $CO_2R$ 
 $CH_3$ 
 $CH_3$ 
 $CO_2R$ 
 $CH_3$ 
 $CO_2R$ 
 $CH_3$ 
 $CO_2R$ 
 $CH_3$ 
 $CO_2R$ 
 $CH_3$ 
 $CO_2R$ 
 $CO_2R$ 

of five methyls derived from S-adenosyl methionine (SAM) to Factor III ( $\underline{3}$ ); (ii) the contraction of the permethylated (seven or eight methyls) macrocycle to corrin; (iii) the extrusion of C-20 and its attached methyl group leading to the isolation of acetic acid (ref. 7, 8 & 4b); (iv) decarboxylation of the acetic acid side-chain in ring C (C-12); and (v) insertion of  $\operatorname{Co}^{2+}$ . In order to justify the continuation of our search for such intermediates whose inherent lability is predictable, we have applied  $^{13}\mathrm{C}$  pulse-labeling methods to the cell-free system from Propionibacterium shermanii (ref. 9), which converts uro'gen III ( $\underline{1}$ ) (ref. 1 & 9) and sirohydrochlorin ( $\underline{2}$ ) (ref.  $\underline{3}$  &  $\underline{10}$ ) to cobyrinic acid ( $\underline{4}$ ), a technique used previously in our laboratory to detect the flux of  $^{13}\mathrm{C}$  label through the intermediates of alkaloid biosynthesis in higher plants (ref. 11).

It was argued that the full methylation cascade could be differentiated in time, provided that enzyme-free intermediates accumulated in sufficient pool sizes to affect the resultant methyl signals in the  $^{13}\text{C}$  NMR spectrum of the target molecule, cobyrinic acid (4), when the cell-free system is challenged with a pulse of  $^{12}\text{CH}_3\text{-SAM}$  followed by a second pulse of  $^{13}\text{CH}_3\text{-SAM}$  (or vice versa) at carefully chosen intervals in the total incubation time (9-10 hr). By this approach it should be possible to "read" the biochemical history of the methylation sequences as reflected in the dilution (or enhancement in the reverse experiment) of  $^{13}\text{CH}_3$  label in the seven methionine-derived methyl groups of cobyrinic acid after conversion to cobester  $(\underline{5})$ , whose  $^{13}\text{C}$  NMR spectrum has been completely assigned (ref. 1, 12 & 13).

The validity of the method was tested in a preliminary experiment using a two-phase system.  $^{13}\text{CH}_3\text{-Methionine}~(90\%\ ^{13}\text{C};~30\ \text{mg})$  was added to a whole-cell (100 g) suspension of P. shermanii in phosphate buffer containing  $\delta\text{-aminolevulinic}$  acid (20 mg), in the absence of  $\overline{\text{Co}^{2+}}$ . Under these conditions the cells produce uro'gen III (1), sirohydrochlorin (2), and Factor III (3), but no corrin. Cell disruption and incubation of the extract (ref. 10) with added  $\text{Co}^{2+}$  and pulses of  $^{12}\text{CH}_2\text{-SAM}$  at varied time intervals was monitored for differential methylation by isolation of cobyrinic acid, conversion to cobester (5), extensive purification, and finally  $^{13}\text{C}$  NMR analysis of the enriched samples (normally 50-150 µg). Optimization of these conditions led to the spectrum shown in Fig. 1, which reveals a clear distinction between the peak heights of the seven methyl groups of cobester when compared with a spectrum obtained by adding  $^{13}\text{CH}_3\text{-SAM}$  at the outset. The high relative intensities of the C-2 and C-7 signals bear testimony to the initial formation in whole cells of the 2,7-dimethyl isobacteriochlorin, sirohydrochlorin (2), in the absence of  $\text{Co}^{2+}$ . The differential dilution of methyl intensity in cobester not only suggests that free intermediates have accumulated, but that even in this qualitative experiment, the sequence of methylation is revealed as C-2  $\approx$  C-7 > C-17 > C-12 $\alpha$  > C-1 > C-5  $\approx$  C-15, since the timing of the addition of  $^{12}\text{CH}_3\text{-SAM}$  dilutes the pool sizes of  $^{13}\text{CH}_3\text{-enriched}$  methylated intermediates in the order in which they are formed. Thus, C-17 is the site of the fourth, C-12 $\alpha$  the fifth, and C-1 the sixth methylation. Note that the experiment does not distinguish C-5 from C-15 (the seventh and eighth methylations) (ref. 14).

Finer tuning of the experiment was achieved in the reversed pulse mode using a porphyrinfree, cell-free system and unlabeled sirohydrochlorin (900  $\mu g)$  (2) as substrate. Incubation with  $^{12}\text{CH}_3\text{-SAM}$  was followed by a pulse of  $^{13}\text{CH}_3\text{-SAM}$  (ref. 15) after an interval (ca. 6 hr) which allowed the accumulation of unlabeled intermediates. The resultant cobester (5) will bear only five enriched methyls, at C-1, C-5, C-12 $\alpha$ , C-15, and C-17. The spectrum shown in Fig. 2a provides striking confirmation and extension of the preliminary experiment in that the relative intensities of C-12 $\alpha$  and C-17 are much lower than that of C-1 which, in turn, is differentiated from C-5 and C-15 (ref. 14), i.e. the pulse of  $^{13}\text{CH}_3\text{-SAM}$  is diluted by an accumulated pool of unlabeled tetra- and pentamethyl intermediates, and becomes available for more efficient labeling of the hexa-  $\rightarrow$  octamethyl intermediates. Control experiments show that very early pulsing (0-60 min) leads to a spectrum of cobester showing approximately equal intensity of all five methyls after "normalization" for C-5 and C-15 (ref. 14) (Fig. 2b), whilst late addition (~9 hr) affords unlabeled cobester. Thus, the complete sequence

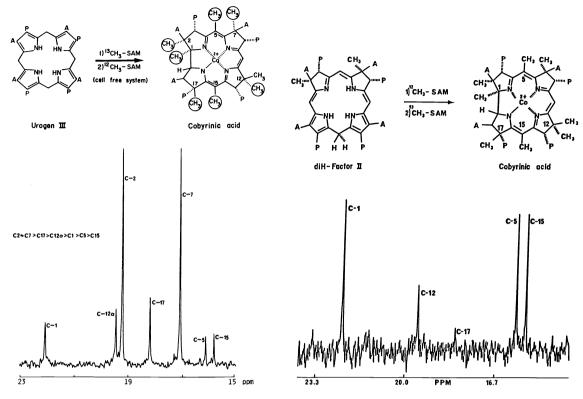


Fig. 1.  $^{13}\text{C}$  NMR spectrum of  $^{13}\text{C}$ -enriched cobester  $(\underline{5})$  (270  $_{\text{$\mu$}}\text{g}$  in 0.5 ml KCN saturated benzene-d $_{6}$ ) isolated from  $\underline{\text{P. shermanii}}$  (see text for incubation details).

Fig. 3. Spectrum of enriched cobester  $(\underline{5})$  (50 µg), accumulated as in Fig. 1 (see text for incubation conditions).

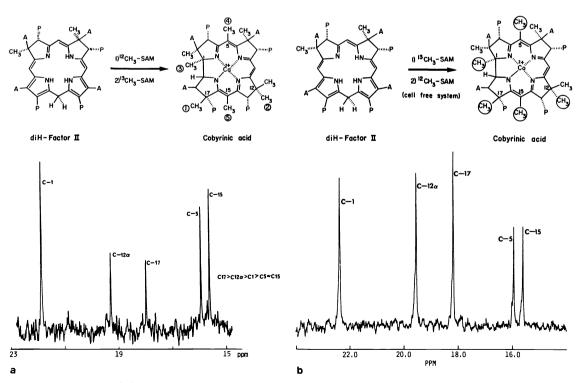


Fig. 2. (a) Spectrum of enriched cobester ( $\underline{5}$ ) (46  $\mu g$ ). (b) Spectrum of enriched cobester ( $\underline{\overline{5}}$ ) (105  $\mu g$ ), accumulated as in Fig. 1.

of methylation of uro'gen III can be described as C-2 > C-7 > C-20 > C-17 > C-12 $\alpha$  > C-1 >  $C-5 \approx C-15$ , a result which complements and extends a report on the differentiation of C-17 as the fourth methylation site in a pulse experiment with extracts of a different bacterium, Clostridium tetanomorphum (ref. 16). On the basis of this sequence, we propose the structures shown in Scheme 2 as the targets of the search for the "missing" intermediates of corrin biosynthesis. For example, the pyrrocorphin structures suggested for Factors 5 and 6 take into account the sequence C-17 methylation, decarboxylation of the C-12 acetate side-chain, and C-12 $\alpha$  methylation. Similarly, the structures of Factors 7 and 8 are proposed to rationalize the methylation of C-1 and the hydration of C-20 as a prelude to the ring contraction/acetic acid extrusion ( $\rightarrow$  Factor 9) for which we have used Eschemmoser's in vitro analogy (ref. 17). The final methyl functionalizations at C-5 and C-15 (in Factor 9) are suggested to follow  $Co^{2+}$  insertion (ref. 1, 18 & 19), since hydrogeno cobyrinic acid is not involved in corrin biosynthesis (ref. 20). A metal complex template — not necessarily  $Co^{4+}$  — may stabilize Factors 4-9. For example, zinc corphinate or pyrrocorphinate structures can be promulgated for Factors 4-8 where M = Zn or  $Zn^+$ , and the loss of acetic acid may well take place from the <u>cobalt</u> complex of Factor 9 based on the work of Nussbaumer and Arigoni (ref. 21). The later steps, however, can only be defined when the intermediates have been discovered. However, the most important implications of the differential incorporations of SAM-derived methyl groups into cobester as a function of time are as follows: (a) Several stable enzyme-free intermediates must accumulate. (b) There appear to be at least five "methylases" responsible for the uro gen-corrin connection. Methylase I (C-2, C-7), which has already been shown (ref. 10) to transform uro'gen III as far as the mono- and dimethyl intermediates Factors I and II (2), methylase II (C-20), methylase III (C-17), and methylase IV and methylase V (C-1, C-5, C-15). (c) The fact that cobalt-deficient cells produce substantial amounts of C-2, C-7, and C-20 methylated intermediates [as (2) and (3)] but insufficient tetra-  $\rightarrow$  octamethyl intermediates to perturb the ratio of methyl labeling in cobester (Fig. 1) suggests that similar pulse experiments with Co<sup>2+</sup> should define the point at which cobalt insertion takes place.

In summary, the experiments described above (ref. 22) suggest that the search for compounds related to the structures suggested in Scheme 2 can now proceed with confidence.

Further refinement of the experiment where the incubation was pulsed with  $^{13}\text{CH}_3\text{-SAM}$  after an interval of only 3-4 hr, afforded a spectrum of cobester  $(\underline{5})$  in which the signal C-17 had almost disappeared, leading to complete differentiation between the methylation times for C-17 (3-4 hr) and C-12 $\alpha$  (4-6 hr) (Fig. 3). This implies that discrete methylating enzymes are involved at these two centers and at C-2/7, C-20, C-1 and C-5/15 (ref. 22), and that, finally, the possibility of isolating the missing factors, perhaps as their complexes with metals other than cobalt, can become a reality.

### DIRECT OBSERVATION OF ENZYME-SUBSTRATE COMPLEXES BY TRITIUM NMR SPECTROSCOPY

The central role of uro'gen III (1) in heme, chlorophyll and corrin biosynthesis has captured and maintained the interest of bioorganic chemists in the mechanism of action of the two enzymes required for the synthesis of (1) from porphobilinogen (PBG;  $\underline{6}$ ). We now describe recent NMR experiments with the first of these enzymes, PBG deaminase (EC 4.3.1.8), which catalyzes the head-to-tail condensation of 4 mol of PBG  $(\underline{6})$  to pre-uro'gen, whose release and stabilization as the (hydroxymethyl)bilane (HMB,  $\underline{12}$ ) has been the subject of extensive investigation (ref. 23-26). HMB may cyclize chemically to uro'gen I  $(\underline{13})$  or serve as the substrate for uro'gen III cosynthetase (EC 4.2.1.75) to form uro'gen  $(\underline{11})$  (Scheme 3).

Deaminase (MW  $\simeq$  36,000) from human sources (ref. 27), Rhodopseudomonas spheroides (ref. 28-30), and Euglena gracilis (ref. 31 & 32) forms stable covalent complexes bearing up to four condensed PBG units. It has been suggested (ref. 27-32) that the amine function at C-11 of PBG is replaced by a nucleophilic "X" group at the active site of deaminase, where X = 0, S or NH to form  $\underline{7-10}$  (Scheme 3). The introduction of  $^{13}$ C enrichment at C-11 should allow observation of the chemical shift for the new CH<sub>2</sub>X group in the region 25-60 ppm. In our hands, experiments using  $[2,11-^{13}C_2]$ PBG to label the complexes  $\underline{7-10}$  provided no  $^{13}$ C NMR evidence for enrichment above natural abundance either in the above complexes or in the proteolytic digests of the mono-PBG complex  $\underline{7}$  (ref. 27, 28 & 33) due to the combination of large line widths and high density of resonances in the region of interest. This result contrasts with a recent claim (ref. 32) for  $^{13}$ C-signal enhancement near 42 ppm, consistent with amine functionality at the active site ( $\underline{7}$ , X = NH). In view of the high natural abundance profile near 40 ppm in the  $^{13}$ C spectrum of deaminase (ref. 32 & 33) and the resultant ambiguity of assignment in the CH<sub>2</sub>X region, we sought a general solution to structural problems in covalent enzyme-substrate complexes where the lack of a "window region" precludes rigorous assignment and now describe the first application of tritium, a nucleus of high sensitivity and low (<10<sup>-16</sup>) natural abundance (ref. 34), as an NMR probe of chemical shift in the environment of a productive covalent complex of enzyme and substrate.

[2,6,6,11,11- $^3H_5$ ]PBG ( $\underline{6a}$ ) (ref. 35) (132 Ci/mmol) was synthesized from [3,3,5,5- $^3H_4$ ]-5-aminolevulinic acid (ALA) (ref. 36) by the action of ALA dehydratase from R. spheroides (ref. 37). The  $^1H$ -decoupled  $^3H$  NMR spectrum of  $\underline{6a}$  (Fig. 4i) confirmed the position of  $^3H$  labeling by comparison with the  $^1H$  NMR spectrum of PBG. The resonances occur at 6.69 (C-2,

CT), 4.15 (C-11, HCT), 2.62 (C-6, HCT), and 2.56 ppm (C-6, CT $_2$ ). The tritiated PBG was rapidly mixed with highly purified (>95%) deaminase (ref. 38) (4000 units (ref. 39)) from R. spheroides and the covalent complexes separated from small molecules by gel filtration on G-50 Sephadex. Analysis of the concentrate by analytical gel electrophoresis showed it to be >90% of the monopyrrole complex (ref. 27 & 28) (7a; 16 mCi). The  $^3\text{H}$  spectrum (Fig. 4ii) of 7a exhibits resonances (ref. 40) at 6.18 (C-2, CT), 3.28  $\pm$  0.1 (pyrrole-CHT-X-Enz), and 2.48  $\pm$  0.1 ppm (pyrrole-CT $_2\text{CH}_2\text{CO}_2\text{H}$ ) at 5.5°C. At 23°C (Fig. 4iii) the signals at 6.18 and 3.28 ppm disappear and are replaced by new resonances at 3.58  $\pm$  0.1 (meso methylenes (CHT) of uro'gen I (13a) and methylenes (CHT) of complexes 8-10, R =  $^3\text{H}$ ), 2.75  $\pm$  0.1 (CT $_2\text{CH}_2\text{CO}_2\text{H}$  of  $^8$ -10, R =  $^3\text{H}$ ), 2.48  $\pm$  0.1 (CT $_2\text{CH}_2\text{CO}_2\text{H}$  of uro'gen I (13a), and 4.69 ppm (HOT, exchanged from  $^8$ -10, R =  $^3\text{H}$ ), 2.48  $\pm$  0.1 (CT $_2\text{CH}_2\text{CO}_2\text{H}$  of uro'gen I (13a) (whose  $^3\text{H}$  chemical shifts are identical with the corresponding CH $_2$  resonances in the  $^1\text{H}$  NMR spectrum) in absence of free PBG is ascribed to disproportionation of complex  $^7\text{a}$  via  $^8$ -10 whose methylene (CHT) and side-chain groups (C-T $_2\text{CH}_2\text{CO}_2\text{H}$ ) can be observed along with those of uro'gen I in the signals at 3.58, 2.75 and 2.48 ppm. Such a disproportionation also accounts for the disappearance of the signal at 3.28 ppm, which would be expected to lose up to 90% of its original intensity, on the basis of the statistical randomization of  $^3\text{H}$  label, from 7a + 8  $\rightarrow$  9  $\rightarrow$  10  $\rightarrow$  13.

To demonstrate the catalytic competence of the monopyrrole complex  $\frac{7}{7}$ , unlabeled PBG (6) was added to the  $^3\text{H}$  complex  $\frac{7}{2}$  at  $3.5^{\circ}\text{C}$  and the formation of uro'gen I monitored by  $^3\text{H}$  NMR. At  $3.5^{\circ}\text{C}$  a transient low-intensity signal was observed at 4.76 ppm, a chemical shift consistent with the vinyl (R) hydrogen of the azafulvene (11a) (ref. 41). On warming to  $23^{\circ}\text{C}$  (Fig. 4iv), sharp resonances for unbound uro'gen I (13a) appeared at 3.58 (20-meso CHT) and 2.48 ppm (propionate CHT) corresponding to the  $^1\text{H}$  chemical shifts in an enzyme-free sample of uro'gen I (ref. 38).

The large line widths of the spectrum in Fig. 4 (spectra ii and iii) (~150-300 Hz) reflect an environment in which the active site of the enzyme is probably buried within the protein. The line width of the propionate side chain also suggests that it is covalently attached or ionically associated with the protein, which is consistent with literature reports on the inhibitory effects of PBG analogues (ref. 42-46). The  $^3$ H chemical shift (3.28  $\pm$  0.1 ppm) of the methylene directly attached to the enzyme allows conclusions to be drawn as to the nature of the nucleophilic group "X" in Scheme 3. That the methylene could be bound to the oxygen

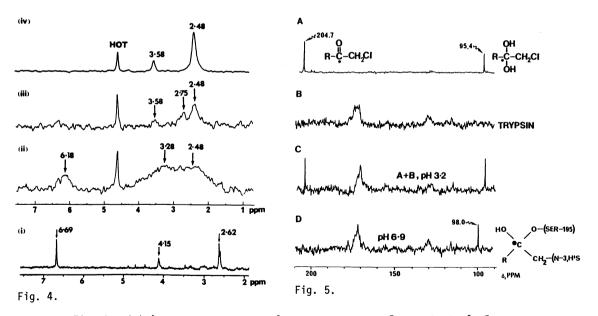


Fig. 4. (i)  $^1\text{H}$ -decoupled 320 MHz  $^3\text{H}$  NMR spectrum of [2,6,6,11,11- $^3\text{H}_5$ ]PBG at pH 8.0, 25°C. (ii)  $^1\text{H}$  decoupled 320 MHz  $^3\text{H}$  NMR spectrum of [2,6,6,11,11- $^3\text{H}_5$ ]PBG deaminase complex at pH 3.0, 5.5°C. (iii) Same as (ii) but at 23°C. (iv) Same as (ii) plus unlabeled PBG (950  $\mu\text{g}$ ) and after 40 min at 3.5°C and 6 hr at 23°C.

Fig. 5. The  $^{13}$ C NMR spectra of (A) N $^{\alpha}$ -carbobenzyloxylsylchloromethylketone (RCOCH $_2$ Cl);  $\bullet$  =  $^{13}$ C, 90 percent enrichment; 47.6 mM (by weight); 1 mM HCl; D $_2$ O, 16.7 percent (by volume); volume, 0.6 ml; 1660 accumulations; pH 3.1; (B-D) 20 mM sodium phosphate; 12.5 percent (by volume) D $_2$ O; 10,000 accumulations; trypsin, 0.28 mM (concentration of fully active enzyme); volume, 8 ml. The RCOCH $_2$ Cl concentrations, pH and enzyme activities were as follows: (B) 0.00 mM, 3.2, 100 percent; (C) 0.38 mM, 3.2, 100 percent; (D) 0.37 mM, 6.9, 0.06 percent.

of a serine residue is ruled out, since HMB (12) and its methyl ether have chemical shifts of 4.4 and 4.2 ppm, respectively (ref. 38). Model studies (ref. 47) predict  $\delta$  3.9 for methylene attached to amine while the observed value (3.28  $\pm$  0.1 ppm) is more consistent (ref. 49) with a thioether linkage (7, X = S). We therefore suggest that the active-site nucleophilic group in deaminase is a cysteine thiol residue or, less probably, an amino group (7, X = NH) which on covalent binding to C-ll of PBG leads to an upfield shift of ~0.6 ppm from the anticipated value of 3.9 ppm. The former possibility is supported by the observation that deaminase is reversibly inhibited by sulfhydryl blocking reagents (ref. 50).

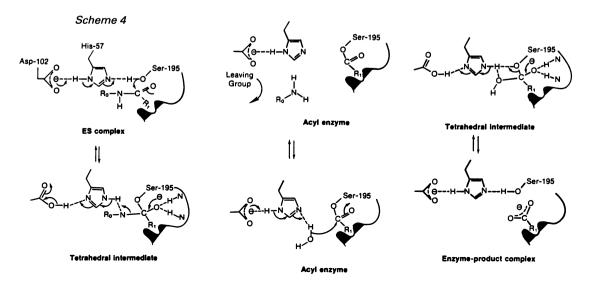
The example of deaminase discussed above (ref. 51) represents a specific and unique case of stabilization of a productive intermediate due to insufficiency of substrate. We now discuss the more general and technically more difficult problem of studying enzyme mechanism by direct NMR methods.

To test this suggestion trypsin was inhibited with the highly specific reagent N $^{\alpha}$ -carbobenzyloxylsylchloromethylketone (ref. 54) (RCOCH $_2$ Cl), labeled in the ketone carbon with 90%  $^{13}\text{C}$ , for it was predicted that a tetrahedral adduct, if formed, would be directly observable by this technique. In aqueous solution (Fig. 5A), RCOCH $_2$ Cl exists as a mixture of the ketone ( $\delta$  = 204.7 ppm) and its hydrate ( $\delta$  = 95.4 ppm). At ph 3.2 no alkylation or inhibition of the enzyme is observed and the spectrum of [ $^{13}\text{C=0}$ ]RCOCH $_2$ Cl is unperturbed (Fig. 5, B and C), showing that at low pH there is no detectable binding or tetrahedral adduct formation prior to alkylation. At pH 6.9 there is rapid, irreversible inhibition, and resonances due to both [ $^{13}\text{C=0}$ ]RCOCH $_2$ Cl and its hydrate are replaced by a single resonance at 98.0 ppm (Fig. 5D), an indication that the  $^{13}\text{C-enriched}$  carbonyl of the inhibitor is tetrahedrally coordinated in the inhibitor-enzyme adduct. Denaturation of the trypsin led to reappearance of a carbonyl resonance (205.5 ppm) and a decrease in the intensity of the resonance at 98.0 ppm. This demonstrates that the tetrahedral adduct formed by the attack of the serine hydroxyl on the inhibitor carbonyl and characterized by the resonance at 98.0 ppm requires an intact trypsin structure (ref. 55).

#### STUDYING ENZYME MECHANISM BY 13C NMR

Almost all enzymatic processes utilize multistep reactions during catalysis, and the characterization of each of these stages is essential if one is to understand enzyme mechanism at the molecular level. Earlier investigators have used spectrophotometric methods for characterizing enzyme-catalyzed reactions, whereas inhibitors that form stable "transition state analogues" have been examined by other techniques that require long periods of data accumulation, for example, X-ray analysis. However, the advent of NMR and its subsequent use in enzymology are beginning to provide a novel and penetrating probe for elucidating enzyme mechanism by directly characterizing intermediates formed in catalysis. The studies of "transition state analogues" allow access to the unique properties of enzymes that enable them to stabilize labile intermediates and therefore achieve their remarkable catalytic efficiency. We discuss first the structures of an enzyme-inhibitor adduct of the serine protease — trypsin — and compare the results of direct observation by  $^{13}\mathrm{C}$  NMR with the structural information inferred by more classical techniques. We then review the powerful combination of NMR and cryoenzymology. The development of this technique, whereby enzyme-catalyzed reactions are studied at subzero temperatures in aqueous organic solvents (cryosolvents), allows such reactions to be slowed down and can prolong the lifetime of enzyme-substrate intermediates (ref. 52).

Scheme 4 shows the generally accepted mechanism for the hydroylsis of an amide function by a serine protease and is representative of the mechanism for all the hydrolyses. To confirm



this mechanistic pathway, the visualization and rigorous characterization of productive tetrahedral intermediates and acyl enzymes by  $^{13}\mathrm{C}$  NMR is the ultimate goal, and we now discuss the progress made so far, particularly with the serine and thiol proteases.

In the domain of synthetic inhibitors, chloromethylketone derivatives of specific substrates are potent irreversible covalent inhibitors of the serine proteases, alkylating the active-center histidine at N-2 (see Scheme 4). X-ray crystallographic studies (ref. 53) led to the suggestion that, in addition to the above alkylation, there was also nucleophilic attack by the active-center serine hydroxyl to form a hemiketal, which is stereochemically analogous to the tetrahedral intermediate purported to occur during catalysis.

In the above experiments with  $[^{13}\text{C=0}]RCOCH_2\text{Cl}$  and trypsin, it is difficult to discount the possibility that the resonance at 98.0 ppm could result from hydration of the carbonyl of the covalently bound inhibitor. However, the use of  $^{18}\text{O}$  isotopic shifts on the  $^{13}\text{C}$  spectrum of the tetrahedral adduct has now shown the adduct is indeed formed by nucleophilic attack of the Ser $^{195}$  hydroxyl group (ref. 56).

### THE QUEST FOR TRUE INTERMEDIATE STRUCTURE: CRYOENZYMOLOGY

The detection and characterization of a productive acyl intermediate by  $^{13}\text{C}$  NMR during catalysis with natural substrates at ambient temperatures is not possible at present, because there is an inherent lack of sensitivity in  $^{13}\text{C}$  NMR spectroscopy. Therefore, the lifetimes of these intermediates must be extended into the domain of the NMR experiment. One approach is to use synthetic substrate analogues which deacylate slowly. Another is to utilize low-temperature cryoenzymological techniques to extend the lifetimes of intermediates.

Since the  $^{13}\text{C}$  resonances of the carbonyl carbon of thioesters are shifted (\$\Delta\$ 20 to 30 ppm) upfield relative to their oxygen analogues (\$\delta\$  $\approx$  165 to 185 ppm),  $^{13}\text{C}$  NMR spectroscopy should allow the direct monitoring of the formation and decay of a thioacyl intermediate. Using [\$^{13}\text{C=0}\$]N-benzoylimidazole (\$\delta\$ = 168.7 ppm), we were able to observe directly a thioacyl intermediate at \$\delta\$ = 195.9 ppm in the presence of papain under the cryoenzymological conditions of \$-6^{\circ}\text{C}\$ in 25 percent aqueous dimethyl sulfoxide (ref. 57) (Fig. 6). Moreover, the thioacyl species is clearly a productive intermediate since the decrease in its signal intensity was accompanied by an increase in the product resonance and by release of free enzyme (half-life, \$\approx96\$ min) determined by titration of its thiol group. The line width of the resonance at 195.9 ppm was 25 + 5 Hz.

$$R-S-C \xrightarrow{\bullet} + H_2O \xrightarrow{\bullet} RS^- + \xrightarrow{\bullet} COOH$$

RSH = Papain

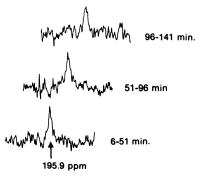


Fig. 6. Reaction of 1.7 mM papain (72 per cent active enzyme), 5.4 mM potassium chloride, 25 percent (by volume) dimethyl sulfoxide, 0.1 M sodium formate buffer (pH 4.1), and 23.6 mM benzoylimidazole. [13C=0]-Benzoylimidazole was added at 0°C; after 15 min the reaction was cooled to -6°C, and the NMR data acquisition commenced 6 min after the reaction was initiated.

The trypsin-catalyzed hydrolysis (Fig. 7) of the highly specific substrate  $N^{\alpha}$ -carbobenzyloxy-L-lysine-p-nitrophenylester (Z-lys-pNP) has been studied in detail under cryoenzymological conditions by both spectrophotometry (ref. 58) and  $^{13}\text{C}$  NMR spectroscopy (ref. 59). The kinetic data from both techniques confirm that the kinetics and mechanism under cryoenzymological conditions are essentially the same as those determined at ambient temperatures by rapid reaction techniques. The hydrolysis of [l- $^{13}\text{C}$ ]Z-lys-pNP (S in Fig. 7A,  $\delta$  = 173.6 ppm) by trypsin was monitored by the decrease in intensity of this signal and the increase in the signal arising from the product (P $_2$  in Fig. 7A,  $\delta$  = 177.7 ppm) at -21°C in 41 percent aqueous dimethyl sulfoxide (Fig. 7). The continued formation of product (P $_2$ ) after all the substrate has been consumed (Fig. 7B) provides indirect evidence for an enzyme bound intermediate whose line width is much greater than that of the free substrate or product and is therefore not directly observable in the individual  $^{13}\text{C}$  NMR spectra of Fig. 7. Improvement

A 
$$NO_{2}$$
 $\delta 173.6$ 
 $E-Ser-OH + C - CH(CH_{2})_{4}NH_{3}$ 
 $\delta 177.7$ 
 $\delta 195$ 
 $E-Ser-OH + HO_{2}CCH(CH_{2})_{4}NH_{3}$ 
 $\delta 177.7$ 
 $\delta 177.$ 

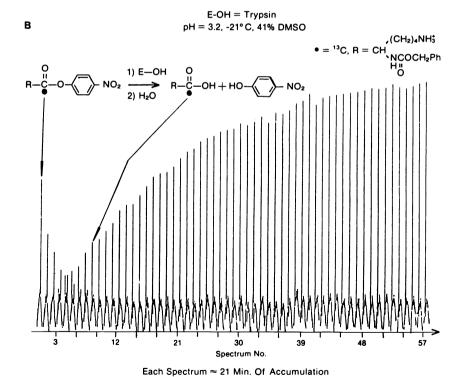


Fig. 7. (A) Reaction of  $[1^{-13}C]Z$ -lys-pNP, 0.83 mM; active trypsin, 0.7 mM; 1 mM HCl (apparent pH, 3.2); and 40 percent (by volume) dimethyl sulfoxide (sample volume, 10 ml; sample temperature, -21°C); NHZ, carbobenzyloxy-. The reaction was initiated by the addition of  $[1^{-13}C]Z$ -lys-pNP; after mixing ( $\approx$ 1 min) NMR data acquisition (B) commenced within 3 min. Each spectrum (1 to 58) represents 10,000 accumulations (time per spectrum, 41 min) recorded sequentially (ref. 58).

of the signal-to-noise ratio by summation of sets of the individual spectra in Fig. 7 made it possible to use difference techniques and allowed direct observation (Fig. 8B) at -21°C of a resonance ( $\delta$  = 176.5 ppm) that was assignable to the acyl enzyme on the basis of its chemical shift and the kinetics of its breakdown formation. Experiments at -1.5°C (Fig. 8A) showed that the acyl intermediate was much more readily detected at this higher temperature, the resonance being clearly resolved in individual spectra as a result of the smaller line width of the resonance at -1.5°C compared to that at -21°C (22  $\pm$  3 Hz and 100  $\pm$  10 Hz, respectively). This illustrates one of the main difficulties of a combined NMR-cryoenzymological approach in which the line width of enzyme-bound species increases dramatically as the cryosolvent viscosity increases on lowering the temperature.

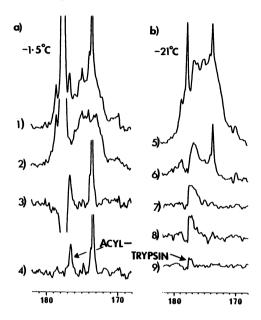


Fig. 8. The  $^{13}$ C NMR spectra of the reaction of [1- $^{13}$ C]Z-1ys-pNP, 1.8 mM; active trypsin, 0.64 mM; 1 mM HCl (apparent pH, 3.02); and 40 percent (by volume) dimethyl sulfoxide (sample volume, 10 ml; sample temperatures (a) -1.5°C and (b) -21°C).

#### SOLID-STATE NMR AS A PROBE FOR ENZYME-SUBSTRATE STRUCTURE

The basis for all of the NMR studies with proteases has relied heavily on the crystal structure determination of the enzyme and/or enzyme complex at the active site (ref. 60). Since the phase change from solid to solution may well involve considerable conformational alteration, the correlation of the two physical methods (X-ray, NMR) in the same phase would be a desirable objective in furthering our understanding of enzyme mechanism. Our final theme concerns the application of solid state cross polarized magic angle spinning (CPMAS) NMR spectroscopy to the direct observation of the hydrolysis of a slow (pseudo) substrate catalyzed by an enzyme. Magic angle spinning (MAS) NMR has already been shown to be a powerful technique for the study of solids generally (ref. 61) and has been used extensively on inorganic systems (ref. 62).

The crystal structures of several complexes of the metalloenzyme, carboxypeptidase  $A\alpha$  (CPA) (EC 3.4.17.1), have been examined in considerable detail. The structure of the complex with glycyl tyrosine (Gly-Tyr) has been refined to 2.0 Å resolution (ref. 63 & 64) and reveals inter alia interactions between the amide nitrogen and the hydroxyl of tyrosine-248 (Tyr-248) (Fig.  $\overline{9A}$ ). The proposed mechanisms for hydrolysis of peptide and ester bonds by CPA have relied heavily on these crystal structures, but a clear distinction between the possible roles of glutamate-270 (Glu-270) in nucleophilic attack either by general base catalysis (Fig. 9A) or by covalent anhydride formation (Fig. 9B) remains a major unresolved problem. Indeed, it is not yet certain whether esters and amides are hydrolyzed by CPA via identical mechanisms (ref. 65).

Gly-Tyr was synthesized as both the  $[^{13}\text{C}]$ -amido (90 atom % enrichment) and amido- $[^{13}\text{C},^{15}\text{N}]$  (90 atom % and 99 atom % enrichment, respectively) isotopomers by known methods (ref. 66). CPA, purchased from Sigma as a suspension in toluene, was crosslinked (ref. 67) and soaked with Gly-Tyr as described previously (ref. 63) and the washed, dried crystals examined by solid-state NMR. The  $^{13}\text{C}$  CPMAS NMR spectrum of the  $^{13}\text{C}$ -enriched Gly-Tyr (Fig. 10A) displays

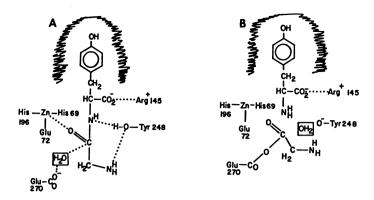
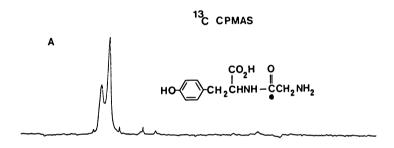


Fig. 9. (A) represents Gly-Tyr bound to CPA showing the indirect attack of Glu-270 promoting the attack of a water molecule on the substrate's amido carbonyl group polarized by interaction with zinc. (B) represents direct attack of Glu-270 on the substrate's amido carbonyl forming an anhydride.



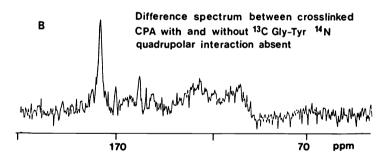


Fig. 10. 25.15 MHz solid-state  $^{13}$ C CPMAS spectrum of (A) amido- $[^{13}$ C]Gly-Tyr,  $\bullet$  =  $^{13}$ C, and (B) the difference CPMAS spectrum of CPA and CPA/ $[^{13}$ C-amido]Gly-Tyr complex.

residual (ref. 68)  $^{13}\text{C-}^{14}\text{N}$  quadrupolar coupling ( $\delta$  = 176 ppm). However, the  $^{13}\text{C}$  CPMAS difference spectrum of CPA and the CPA/Gly-Tyr complex (Fig. 10B) displays a <u>single resonance</u> ( $\delta$  178 ppm, LW<sub>L</sub> 60 Hz) revealing that, under the experimental conditions, the peptide bond of this slow reacting substrate has been cleaved to the extent of >90%. In order to confirm this result, doubly labeled amido-[ $^{13}\text{C}$ , $^{15}\text{N}$ ]Gly-Tyr (Fig. 11A) was bound to CPA under identical conditions and the complex examined by  $^{15}\text{N}$  CPMAS NMR spectroscopy. As can be seen from Fig. 11A, the  $^{15}\text{N}$  resonance of the substrate ( $\delta$  120 ppm) is sufficiently broad (LW<sub>L</sub> 325 Hz) to conceal the  $^{15}\text{N}$ -13C one-bond scalar coupling (J = 16 Hz). In the enzyme complex (Fig. 11C), the observed  $^{15}\text{N}$  resonances correspond to the amide region of CPA (see Fig. 11B;  $\delta$  122 LW<sub>L</sub> = 400 Hz) and an amine (ref. 69) ( $\delta$  42 ppm LW<sub>L</sub> = 250 Hz), respectively. We infer from these experiments that we are observing either the first stable intermediate of the catalytic pathway, i.e. the anhydride of the caleaved glycine residue bound covalently to Glu-270 (Fig. 9B), or the bound glycine accompanied in either case by the second product, tyrosine (Fig. 11D), also bound to CPA, since in a separate experiment it could be shown that no unbound tyrosine or glycine was present in the complex. A distinction between the two glycine species (anhydride or acid) cannot be made in this experiment since the  $^{13}\text{C}$  chemical

764

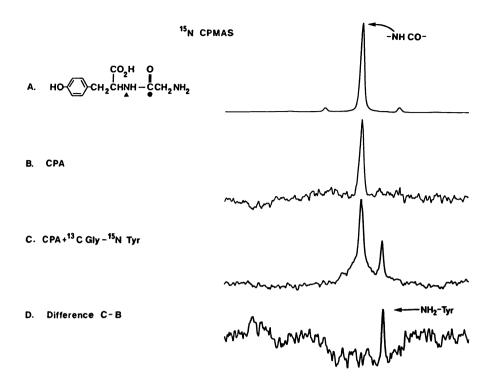


Fig. 11. 20.28 MHz solid-state  $^{15}N$  CPMAS spectrum of (A) amido- $[^{13}C, ^{15}N]$ -Gly-Tyr,  $\bullet$  =  $^{13}C$ ,  $\blacktriangle$  =  $^{15}N$ , (B) CPA, and (C) CPA + amido- $[^{13}C, ^{15}N]$ Gly-Tyr.

shifts of the carbonyl(s) in both the anhydride and the acid are within the observed chemical shift range. The distinction is, however, realized by the use of FT-IR difference spectroscopy which indicates that, at least after several days, no anhydride (Fig. 9B) is present. However, these preliminary experiments clearly indicate the feasibility of simultaneous X-ray and CPMAS NMR studies, especially with slow substrates. In summary, a method of some generality for reaching the long-sought correlation between X-ray diffraction data, the resultant geometry of a substrate undergoing slow catalysis, and the corresponding NMR chemical shifts for selected atoms in the enriched substrate, obtained under identical conditions, is now available through the use of the CPMAS technique which can be further complemented by FT-IR difference spectroscopy.

From the discussion presented in this section, it is clear that the stage is now set for intensive research into the mechanism of enzyme action with cryoenzymology. Although most of the enzymes discussed above lie in the molecular weight range of 20,000 to 35,000, an upper figure of  $\sim 50,000$  probably represents the maximum convenient size for  $^{13}\text{C}$  NMR studies on currently available superconducting instruments with substrates and inhibitors.

Finally, we can expect exciting developments in the application of  $^{13}$ C solid-state NMR spectroscopy to structural problems in enzyme complexes, a field which, although still in its infancy, already shows considerable promise (ref. 70).

#### **Acknowledgements**

We thank the S.E.R.C. (U.K.), the National Institutes of Health and the Robert A. Welch Foundation for generous support at Edinburgh and Texas A&M Universities, and also N.A.T.O. for providing an exchange program with our colleague Professor G. Müller (Stuttgart).

#### **REFERENCES**

A. I. Scott in <u>Vitamin B<sub>12</sub></u> (B. J. Zagalak and W. Friedrich, eds.), p. 247, Walter de Gruyter & Co., Berlin/New York (1979); A. R. Battersby and E. McDonald in <u>Vitamin B<sub>12</sub></u> (D. Dolphin, ed.), p. 107, Wiley, New York (1982).

(D. Dolphin, ed.), p. 107, Wiley, New York (1982).

2. K.-H. Bergman, R. Deeg, K. D. Gneuss, H.-P. Kriemler and G. Müller, Z. Physiol. Chem. 358, 1315 (1977); M. Imfeld, D. Arigoni, R. Deeg and G. Müller in Vitamin B<sub>12</sub> (B. J. Zagalak and W. Friedrich, eds.), p. 315, Walter de Gruyter & Co., Berlin/New York (1979).

- 3. A. I. Scott, A. J. Irwin, L. M. Siegel and J. N. Shoolery, <u>J. Am. Chem. Soc</u>. <u>100</u>, 316 and
- 7987 (1978); A. R. Battersby, E. McDonald, H. Morris, M. Thompson, D. C. Williams, V. Ya. Bykhovsky, N. Zaitseva and V. Bukin, Tetrahedron Lett., 2217 (1977); A. R. Battersby, E. McDonald, M. Thompson and V. Ya. Byhovsky, J. Chem. Soc. Chem. Commun., 150 (1978).

  4. (a) G. Müller, K. D. Gneuss, H.-P. Kriemler, A. I. Scott and A. J. Irwin, J. Am. Chem. Soc. 101, 3655 (1979). (b) G. Müller, K. D. Gneuss, H.-P. Kriemler, A. J. Irwin and A. I. Scott, Tetrahedron (Suppl) 37, 81 (1981). (c) A. R. Battersby, G. W. J. Matcham, E. McDonald, R. Neier, M. Thompson, W. -D. Woggen, V. Ya. Bykhovsky, and W. D. Mongier. E. McDonald, R. Neier, M. Thompson, W.-D. Woggon, V. Ya. Bykhovsky and H. R. Morris, J. Chem. Soc. Chem. Commun., 185 (1979). (d) N. G. Lewis, R. Neier, G. W. J. Matcham, E. McDonald and A. R. Battersby, Ibid, 541 (1979).
- 5. Isolation and refeeding experiments have recently shown that sirohydrochlorin (2) most probably enters the biochemical pathway at the dihydro level, although reisolated and reincorporated as the fully aromatized macrocycle. See A. R. Battersby, K. Frobel, F. Hammerschmidt and C. Jones. <u>J. Chem. Soc. Chem. Commun.</u>, 455 (1982).
- 6. Allusion to these efforts in Cambridge and Texas has been made by A. R. Battersby and by A. I. Scott, see refs. 1 and 16.
- 7. L. Mombelli, C. Nussbaumer, H. Weber, G. Müller and D. Arigoni, Proc. Natl. Acad. Sci., USA 78, 9 (1981).
- A. R. Battersby, M. J. Bushell, C. Jones, N. G. Lewis and A. Pfenninger, Proc. Natl. Acad. Sci., USA 78, 13 (1981).
   A. I. Scott, C. Yagen and E. Lee, J. Am. Chem. Soc. 95, 5761 (1973).
- 10. G. Müller in <u>Vitamin B<sub>12</sub></u> (B. J. Zagalak and W. Friedrich, eds.), p. 279, Walter de Gruyter & Co., Berlin/New York (1979).

  11. A. I. Scott, P. B. Reichardt, M. B. Slaytor and J. G. Sweeny, <u>Bioorg. Chem.</u> 1, 157 (1971).
- 12. L. Ernst, Liebigs Ann. Chem., 376 (1981).
- 13. A. R. Battersby, C. Edington, C. J. R. Fookes and J. M. Hook, J. Chem. Soc. Perkin Trans. <u>1</u>, 2265 (1982).
- 14. In order to acquire a good signal/noise ratio in the minimum time ( $\sim$ 16 hr), a pulse repetition rate of 0.7 sec was used to obtain the spectra shown in Fig. 1 and 2. This has the effect of reducing the relative intensities of the C-5 and C-15 methyl signals by about 30-40% due to the long  $T_1$ 's for  $C_5$  and  $C_{15}$  (1.27 and 1.31 sec, respectively).
- This factor is included in our discussion of the sequence of methylation.

  15. M. F. Hegazi, R. T. Borchardt, S. Osaki and R. L. Schowen in Nucleic Acid Chemistry (L. B. Townsend and R. S. Tipton, eds.), p. 889, Wiley, New York (1978).
- 16. H. C. Uzar and A. R. Battersby, <u>J. Chem. Soc. Chem. Commun.</u>, 1204 (1982). 17. V. Rasetti, A. Pfaltz, C. Kratky and A. Eschenmoser, <u>Proc. Natl. Acad. Sci. USA</u> 78, 16 (1981).
- 18. Based on the concept that cobalt-free corrins exist in Nature (ref. 19).
- 19. For alternative mechanisms and a discussion of cobalt insertion, see A. I. Scott, Pure

- Appl. Chem. 53, 1215 (1981).

  20. T. E. Podschun and G. Müller, Angew. Chem. 97, 63 (1985).

  21. C. Nussbaumer and D. Arigoni, see ETH Diss. #7623.

  22. A. I. Scott, N. E. Mackenzie, P. J. Santander, P. E. Fagerness, G. Müller, E. Schneider,
- R. Sedlmeier and G. Wörner, <u>Bioorg. Chem.</u> 12, 356 (1984).

  23. G. Burton, P. E. Fagerness, S. Hosozawa, P. M. Jordan and A. I. Scott, <u>J. Chem. Soc. Chem. Commun.</u>, 202 (1979); P. M. Jordan, G. Burton, H. Nordlöv, M. M. Schneider, L. Pryde and A. I. Scott, <u>Ibid</u>, 204 (1979).
- 24. A. R. Battersby, C. J. R. Fookes, G. W. J. Matcham, E. McDonald and (in part) K. E.
- Gustafson-Potter, <u>J. Chem. Soc. Chem. Commun.</u>, 316 (1979). 25. A. R. Battersby, C. J. R. Fookes, E. McDonald and G. W. J. Matcham, <u>Bioorg. Chem. 8</u>, 451 (1979).
- 26. A. I. Scott, G. Burton, P. M. Jordan, H. Matsumoto, P. E. Fagerness and L. M. Pryde, J. Chem. Soc. Chem. Commun., 384 (1980).
- 27. P. M. Anderson and R. J. Desnick, J. Biol. Chem. 255, 1993 (1980). 28. P. M. Jordan and A. Berry, <u>Biochem. J. 195</u>, 177 (1981).
- 29. A. Berry, P. M. Jordan and J. S. Seehra, FEBS Lett. 129, 220 (1981).
- 30. J. N. S. Evans, G. Burton and A. I. Scott, unpublished results.
- A. R. Battersby, C. J. R. Fookes, G. W. J. Matcham, E. McDonald and (in part)
   R. Hollenstein, J. Chem. Soc. Perkin Trans. 1, 3031 (1983).
   A. R. Battersby, C. J. R. Fookes, G. Hart, G. W. J. Matcham and P. S. Pandey, J. Chem.
   Soc. Perkin Trans. 1, 3041 (1983).
- 33. See ref. 38 for details for the preparative procedures for complex formation.
  34. J. A. Elvidge, "Synthesis and Applications of Isotopically Labeled Compounds," in Proceedings of an International Symposium, Kansas City, MO, June, 1982 (W. P. Duncan and A. B. Susan, eds.) pp 35-44 and references therein, Elsevier, Amsterdam (1983).
- 35. The  $[^3H]PBG$  employed contains all multiply tritiated species up to the fully tritiated  $[2,6,6,11,11-3H_5]$ PBG but consisted mainly of  $[2-3H_1,6,6-3H_2,11-3H_1]$ PBG.
- 36. Prepared by New England Nuclear by custom tritiation according to our directions
- 37. J. N. S. Evans and A. I. Scott, unpublished results.
- 38. J. N. S. Evans, Ph.D. Thesis, University of Edinburgh, 1985.

- 39. One unit is defined as the amount of enzyme required to consume 1 μmol PBG per hr.
- 40.  $^{3}$ H NMR referencing was performed as follows: A  $^{1}$ H NMR spectrum of [2,6,6,11,11- $^{3}$ H<sub>5</sub>]PBG the chemical shifts of subsequent spectra.
- 41. H. Falk and T. Schlederer, Monatsh. Chem.  $\underline{112}$ , 501 (1981). Interestingly, no NMR evidence for the accumulation of HMB ( $\underline{12a}$ ) was obtained under these conditions involving high concentration (1 mM) of pure deaminase, 3.5°C, pH 8.0 (cf. ref. 23-26).

42. R. B. Frydman and G. Feinstein, Biochim. Biophys. Acta 350, 358 (1974).

43. L. Bogorad, Plant Physiol. 32, xli (1975).

44. L. Bogorad in Comparative Biochemistry of Photoreactive Systems (M. B. Allen, ed.),

- p. 227, Academic Press, New York (1960).
  45. A. T. Carpenter and J. J. Scott, Biochim. Biophys. Acta 52, 195 (1968).
  46. H. Heath and D. S. Hoare, Biochem. J. 72, 14 (1959); H. Heath and D. S. Hoare, Ibid 73, 679 (1959).
- 47. PBG  $(\underline{6})$  displays a resonance at 4.16 ppm for the C-11 methylene protons and shifts 0.05 ppm upfield on deprotonation (ref. 38). The (aminomethyl)bilane ( $\frac{12}{2}$  where  $CH_2OH = CH_2NH_2$ ) displays a resonance at 3.92 ppm at pH 12 (ref. 48), which implies a methylene chemical shift of 3.97 ppm at pH 8.0.
- 48. H.-O. Dauner, G. Gunzer, I. Heger and G. Müller, Hoppe-Seyler's Z. Physiol. Chem. 357, 149 (1976).
- 49. N. E. Mackenzie. H. Rexhausen and A. I. Scott, in press. A model thio ether has  $\delta$  = 3.3 ppm for the  $CH_2$ -S resonance.

50. P. M. Jordan and D. Shemin, J. Biol. Chem. 248, 1019 (1973).

51. J. N. S. Evans, P. E. Fagerness, N. E. Mackenzie and A. I. Scott, J. Am. Chem. Soc. 106, 5738 (1984).

52. P. Douzou, <u>Cryobiochemistry</u>, Academic Press, New York (1977). 53. T. L. Poulos, R. A. Alden, S. T. Frier, J. J. Burktoft and J. Kraut, <u>J. Biol. Chem</u>. <u>251</u>, 1097 (1976).

54. J. R. Coggins, W. Kray and E. Shaw, <u>Biochem. J. 138</u>, 579 (1974). 55. J. P. G. Malthouse, N. E. Mackenzie, A. S. F. Boyd and A. I. Scott, <u>J. Am. Chem. Soc. 105</u>, 1685 (1983).

56. A. I. Scott, N. E. Mackenzie and J. P. G. Malthouse, to be published.

57. J. P. G. Malthouse, M. P. Gamcsik, A. S. F. Boyd, N. E. Mackenzie and A. I. Scott, <u>J. Am. Chem. Soc. 104</u>, 6811 (1982). 58. J. P. G. Malthouse and A. I. Scott, <u>Biochem. J.</u> 215, 555 (1983).

59. N. E. Mackenzie, J. P. G. Malthouse and A. I. Scott, Biochem. J. 219, 437 (1984).

- 60. N. E. Mackenzie, J. P. G. Malthouse and A. I. Scott, Science 225, 883 (1984).
  61. E. R. Andrew, Intl. Rev. Phys. Chem. 1, 195 (1981).
  62. C. A. Fyfe, J. M. Thomas, J. Klinowski and G. C. Gobbi, Angew. Chem., Int. Ed. Engl. 22, 259 (1983).
- W. N. Lipscomb, J. A. Hartsuck, G. N. Reeke, Jr., F. A. Quiocho, P. H. Bethge, M. L. Ludwig, T. A. Steitz, H. Muirhead and J. C. Coppola, <u>Brookhaven Symp. Biol.</u> 21, 24 (1968); W. N. Lipscomb, <u>Acc. Chem. Res.</u> 15, 232 (1982).
   W. N. Lipscomb, G. N. Reeke, <u>Jr.</u>, J. A. Hartsuck, F. A. Quiocho and P. H. Bethge,

- Phil. Trans. Roy. Soc. Lond., Ser. B 257, 177 (1970).
  65. W. N. Lipscomb in "Proceedings of The Robert A. Welch Conferences on Chemical Research. XV. Bioorganic Chemistry and Mechanisms," p. 131 (1971); R. Breslow, J. Chin, D. Hilvert and G. Trainor, Proc. Natl. Acad. Sci. USA 80, 4585 (1983); S. J. Hoffmann, S. S.-T. Chu, H. Lee, E. T. Kaiser and P. R. Carey, J. Am. Chem. Soc. 105, 6971 (1983); L. C. Kuo, J. M. Fukuyama and M. W. Makinen, J. Mol. Biol. 163, 63 (1982).

- 66. J. P. Greenstein and M. Winitz, Chemistry of the Amino Acids, Wiley, New York (1961).
  67. F. A. Quiocho and F. M. Richards, Biochemistry 5, 4062 (1966).
  68. M. H. Frey and S. J. Opella, J. Chem. Soc. Chem. Commun., 474 (1980).
  69. G. C. Levy and R. L. Lichter, Nitrogen-15 Nuclear Magnetic Resonance Spectroscopy, Wiley, New York (1979).
- 70. N. E. Mackenzie, P. E. Fagerness and A. I. Scott, J. Chem. Soc. Chem. Commun., 635 (1985).